



1P3S HIGH FREQUENCY TRANSFORMER BASED DUAL-ACTIVE BRIDGE DC-DC CONVERTER

Murat Mustafa Savrun^{1*}, Tahsin Köroglu², Adnan Tan³, Mehmet Uğraş Cuma¹, Kamil Çağatay Bayindir⁴, Mehmet Tumay¹

¹Electrical-Electronics Engineering Department, Adana Science and Technology University, Faculty of Engineering, TURKEY.

²Automotive Engineering Department, Adana Science and Technology University, Faculty of Engineering, TURKEY.

³Electrical-Electronics Engineering Department, Cukurova University, Faculty of Engineering and Architecture, TURKEY.

⁴Energy Systems Engineering Department, Yildirim Beyazit University, Faculty of Engineering and Natural Sciences, TURKEY.

Abstract

The dual active bridge DC-DC converter topology gains developing application area in renewable energy systems, electric vehicles, power quality devices etc. due to its structural and functional advantages.

In this paper, a new dual active bridge (DAB) based DC-DC converter equipped with an isolated high-frequency transformer with 1 primary / 3 secondary windings is proposed which is composed of three voltage source converter (VSC) in the secondary side and a voltage source converter in the primary side. Each voltage source converters have own dc links. The single phase shift modulation (SPS) method that is the commonly used control method in high power transfer applications is used for each voltage source converters independently to achieve bidirectional power flow of DC-DC converter. The phase shift modulation is implemented by PI controller. The power flow between the dc-links is provided by VSC's own phase shift angles. Moreover, extended phase shift (EPS) modulation and dual phase shift (DPS) modulation is also implemented to the system to control the power flow. Performance comparison of modulation methods is also done in the study. To validate the proposed system, a simulation model has been developed for 10 kVA rating using MATLAB/Simulink. The performance of the proposed system is verified with various case studies.

Key words: *Dual active bridge, H bridge, DC-DC converter, Phase shift modulation*

1. Introduction

Nowadays, the applications of renewable energy sources, electric vehicles, fuel cell energy systems, power quality systems etc. bring into prominence of the bidirectional DC-DC converter (BiDC) applications to eliminate the adverse effect of the unstable voltages and provide bidirectional power flow [1]. For instance, the regenerative braking system of electric vehicle reveals the requirement of bidirectional power flow [2].

In literature, various BiDC topologies have been investigated. These topologies can be classified as non-isolated converters and isolated converters [3-5]. In the non-isolated converter topology, line frequency (50 or 60 Hz) transformers are employed to ensure the galvanic isolation in the aforementioned applications. The line frequency transformers are bulky and costly devices. Isolated converters equipped with high-frequency transformers (HFT) can be used as bidirectional converter [6]. The HFTs are much smaller in volume and cost than line frequency transformers. The isolated BiDC topologies are reviewed in [7]. The well-known topologies of the isolated BiDC are flyback converters [8, 9], forward-flyback converters [10, 11], cuk converters [12], half bridge converters [13, 14] and full bridge (H bridge) converters [15-18].

BiDC topologies are frequently used in DVR applications to reduce the energy storage element requirement and to adjust the voltages of dc-link capacitors during the voltage sag and swell [19-21]. Bidirectional full bridge (dual active bridge) converters have such advantages; high power handling capability and soft switching of the switches [22]. Generally, dual active bridge based DC-DC converter topologies equipped with an isolated high-frequency transformer with 1 primary / 1 secondary windings are used in DVR applications [23, 24]. Therefore, the phases are connected to a common dc-link capacitor. In the proposed topology, the high-frequency transformer with 1 primary / 3 secondary windings provides separate dc-link capacitors for each phase and also provides reduced dc-link capacitor ratings. These advantages are provided by only [25] in the literature. But, unidirectional power flow can be achieved in this study.

The main motivation of the proposed topology is to provide galvanic isolation by using high-frequency transformer rather than line frequency transformers and to provide individual capacitors for each phase. In this paper, a new dual-active bridge based bidirectional DC-DC converter topology equipped with 1 primary / 3 secondary windings HFT is proposed. The dual-active bridge topology has chosen as a converter because of its operational advantages. The proposed converter is equipped with 1 primary / 3 secondary windings HFT to provide the galvanic isolation and separate dc-link capacitors.

The commonly used control methods to control the DAB based BiDC are SPS modulation, EPS modulation and DPS modulation. The SPS modulation method is used more frequently, because it has some advantages, such as small inertia, high dynamic, ease of realizing soft switching control, simple control and wide range power flow [7].

The proposed system capability has been examined in 10 kVA simulation model which is developed using MATLAB/Simulink. The paper is organized in the following manner: the power circuit model of the proposed system is presented in Section 2. In Section 3, the control method is described. The simulation study and result comparisons are presented in Section 4. The conclusion of the paper is given in the final section.

2. Power Circuit of the Proposed System

The proposed system is constituted by high-frequency transformer, four single phase full bridge (i.e. H bridge) voltage source converters, dc link capacitors (V_{S1-2-3}) and auxiliary inductors ($L_{p,1,2,3}$). The H bridges act as a two-level converter and generate square wave on the transformer windings. The switching elements of H bridges are chosen as IGBT because of high switching frequency capability. The switching frequency of the system is determined as 20 kHz. The proposed topology employs a high frequency (20 kHz) transformer to provide galvanic isolation for the converters. The HFT turns ratio is 3:1 because of the determined voltage levels on both sides of the converter. As it can be seen from Figure 1, separate dc links are achieved on the secondary side of the converter by using HFT. Thus, the topology can be assumed as three different dual active bridge converters.

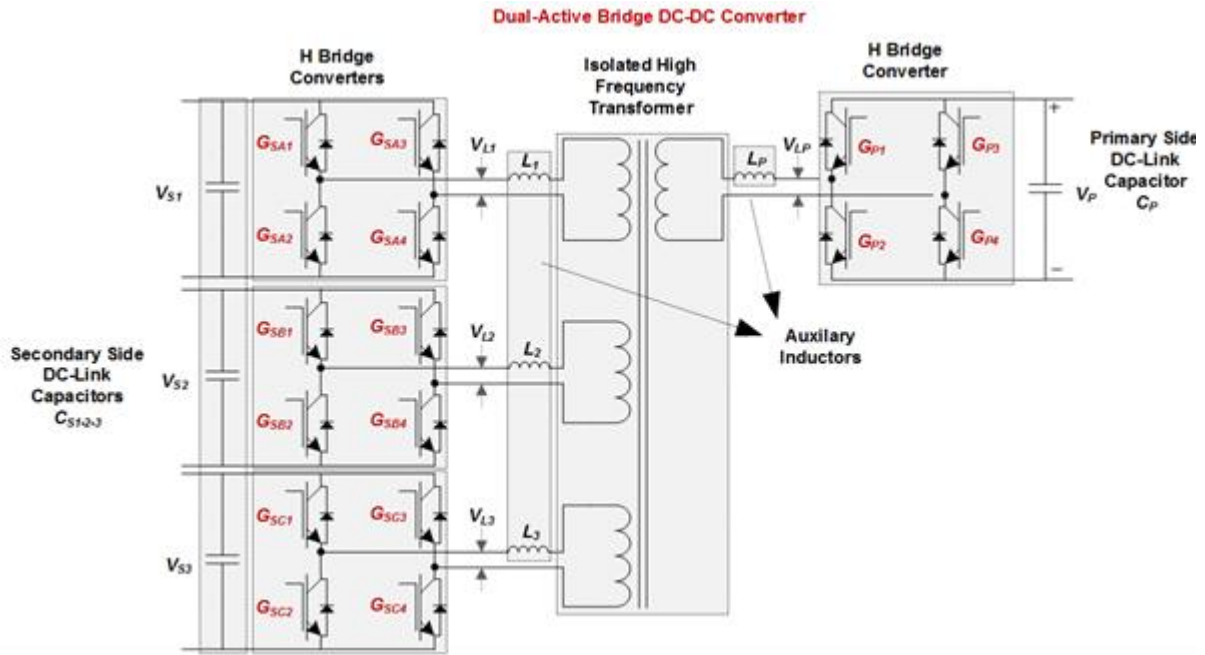


Fig. 1. The proposed system topology.

In the equivalent circuit model of the first DAB converter illustrated in Figure 2, the DAB based BiDC consists of two sources and an inductor that is the total value of transformer leakage inductance and auxiliary inductors. The bidirectional power flow through the total inductor is provided by phase shift angle between the primary side H bridge and the secondary side H bridge. The operation of the system can be simplified as the equivalent circuit with neglecting the effect of the magnetizing inductance. The parameters of the proposed system are listed in Table 1.

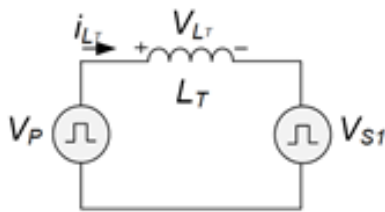


Fig. 2. The equivalent circuit of the first DAB based BiDC.

Table 1. Parameters of the proposed system.

	HFT	Auxiliary Inductors	DC Link Capacitors
Power	10 kVA	$L_{p,S1,2,3}$	50 uH
Primary Voltage (V_P)	540 V		
Secondary Voltage ($V_{S1,2,3}$)	160 V	$C_{p,S1,2,3}$	45/20,20,20 mF
Switching Freq.	20 kHz	H Bridges	
Turns Ratio	3:1	Switching Elements	IGBT

3. Controller of the Proposed System

The controller of the proposed system is designed to provide stable DC link voltages on the secondary side and provide bidirectional power flow. Since the transformer designed in the proposed topology has 3 secondary windings, separate dc link capacitors are achieved on the secondary side. Thus, the controller provides independent control for the secondary side dc links.

In the controller of the system, single phase shift (SPS) modulation method is used. As illustrated in Figure 3, $G_{P1}-G_{P4}$, $G_{P2}-G_{P3}$, $G_{SA1}-G_{SA4}$ and $G_{SA2}-G_{SA3}$ are square wave gate signals of IGBTs. To achieve power flow between the dc-links, the phase shift angle, which is denoted by δ , is adjusted by considering the total inductance (L_T), which is the sum of auxiliary inductors and leakage inductance of HFT. The power transfer P_D can be calculated by using Eq. 1 [1, 26]. The auxiliary inductors control the speed of power flow and power handling capability while providing power transfer. Thus, the inductor values have a significant impact on the power transfer performance of DC-DC converter. The values of the auxiliary inductances are derived from the following formula according to the desired power transfer ratings and phase angles.

$$P_D = \frac{V_{DC} n V_{DVR,DC1}}{\omega L_T} \delta \left(1 - \frac{|\delta|}{\pi}\right) \tag{1}$$

The capacitance values of DC link capacitors are calculated according to the value of power to be transferred. The maximum power transfer rating of the system is determined as 10 kVA and the nominal power handling capacity of each phase is determined as 2.5 kVA.

$$C_{DC} = \frac{2tS}{(V_{dc,i}^2 - V_{dc,f}^2)} \tag{2}$$

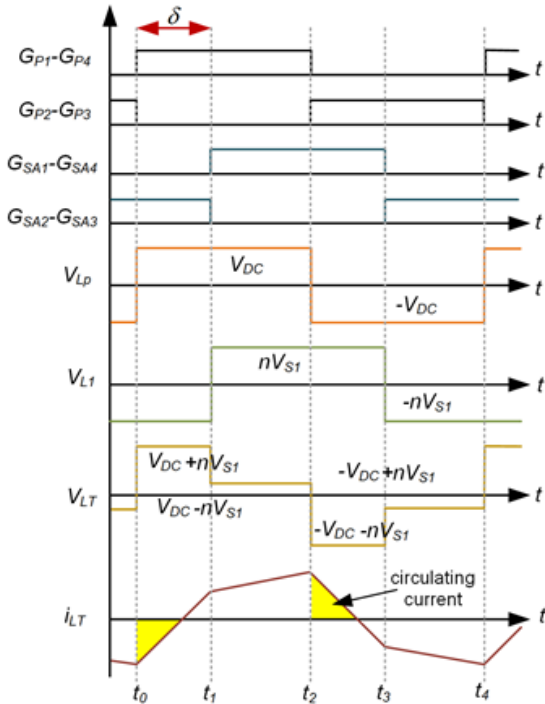


Fig. 3. The SPS control.

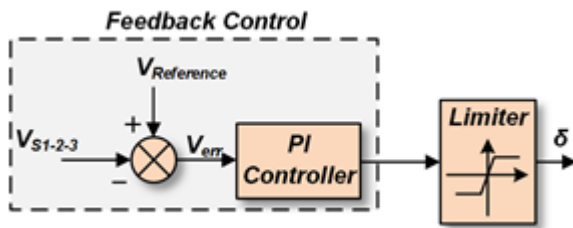


Fig. 4. The dc link voltage control.

S is the transferred apparent power, *t* is duration of the disturbance, $V_{dc,i}^2$ is the initial capacitor voltage and $V_{dc,f}^2$ is the final capacitor voltage.

The simplified theoretical waveforms of the single phase shift control strategy where $V_p > nV_{S1}$ (i.e. the charging of secondary side first DC link capacitor- C_{S1}) is given in Figure 3. Total inductance of the first DAB based BiDC is the sum of L_p , L_{S1} and leakage inductance of HFT.

- t_0-t_1 : During this interval, the switches of GP₁, GP₄, G_{SA2} and G_{SA3} are on, whereas G_{SA1}, G_{SA4}, GP₂ and GP₃ are off. Therefore the V_{Lp} is positive and V_{Li} is negative. So, the voltage across the total inductance (V_{LT}) is positive high, thus the current i_{LT} increases linearly from negative to positive.

- t_1-t_2 : During this interval, the switches of GP₁, GP₄, G_{SA1} and G_{SA4} are on, whereas G_{SA2}, G_{SA3}, GP₂ and GP₃ are off. Therefore the V_{Lp} and V_{Li} are positive. So, the voltage across the total inductance (V_{LT}) is positive low, thus the current i_{LT} continue to increase linearly.

- t_2-t_3 : During this interval, the switches of GP₂, GP₃, G_{SA1} and G_{SA4} are on, whereas G_{SA2}, G_{SA3}, GP₁ and GP₄ are off. Therefore the V_{Lp} is negative and V_{Li} is positive. So, the voltage across the total inductance (V_{LT}) is negative high, thus the current i_{LT} decreases linearly from positive to negative.

- t_3-t_4 : During this interval, the switches of GP₂, GP₃, G_{SA2} and G_{SA3} are on, whereas G_{SA1}, G_{SA4}, GP₁ and GP₄ are off. Therefore the V_{Lp} and V_{Li} are negative. So, the voltage across the total inductance (V_{LT}) is negative low, thus the current i_{LT} decreases linearly.

- t_4- : During this interval, as in the first condition, the switches of GP₁, GP₄, G_{SA2} and G_{SA3} are on, whereas G_{SA1}, G_{SA4}, GP₂ and GP₃ are off. Therefore the V_{Lp} is positive and V_{Li} is negative. So, the voltage across the total inductance (V_{LT}) is positive high, thus the current i_{LT} increases linearly from negative to positive.

The circulating power occurs due to the fact that the input and output voltage is positive when the current of the isolation transformer is negative. The circulating power decreases the efficiency of conversion. Thus, alternative phase shift modulation methods such as EPS modulation and DPS modulation are preferred to increase the efficiency of the conversion by reducing the circulating power through providing three level output voltage on primary side or both primary and secondary sides [17, 27, 28, 29].

The phase shift angles of the H bridges are obtained by a simple PI controller. The measured actual value of dc link voltage is subtracted from the dc link reference voltage and error between the actual dc link voltage and reference is obtained. The error signal is applied to the PI controller and the phase shift angle is determined. The block diagram of the dc link voltage control is presented in Figure 4.

4. Simulation Results of the Proposed System

The main aims of the proposed system are to achieve bidirectional power flow between the dual active bridges and provide isolation between the dc terminals of both primary and secondary sides. The proposed system is investigated with the SPS modulation method. As it can be seen from Figure 5, the secondary side dc links at different voltage levels (120/80/170 V respectively) are charged/discharged simultaneously to the desired reference voltage (160 V) by their own phase shift angles. The controller of the system achieves control of dc links separately. Bidirectional power flow by providing the functions of charging and discharging simultaneously has been also gained with positive and negative phase shift angles.

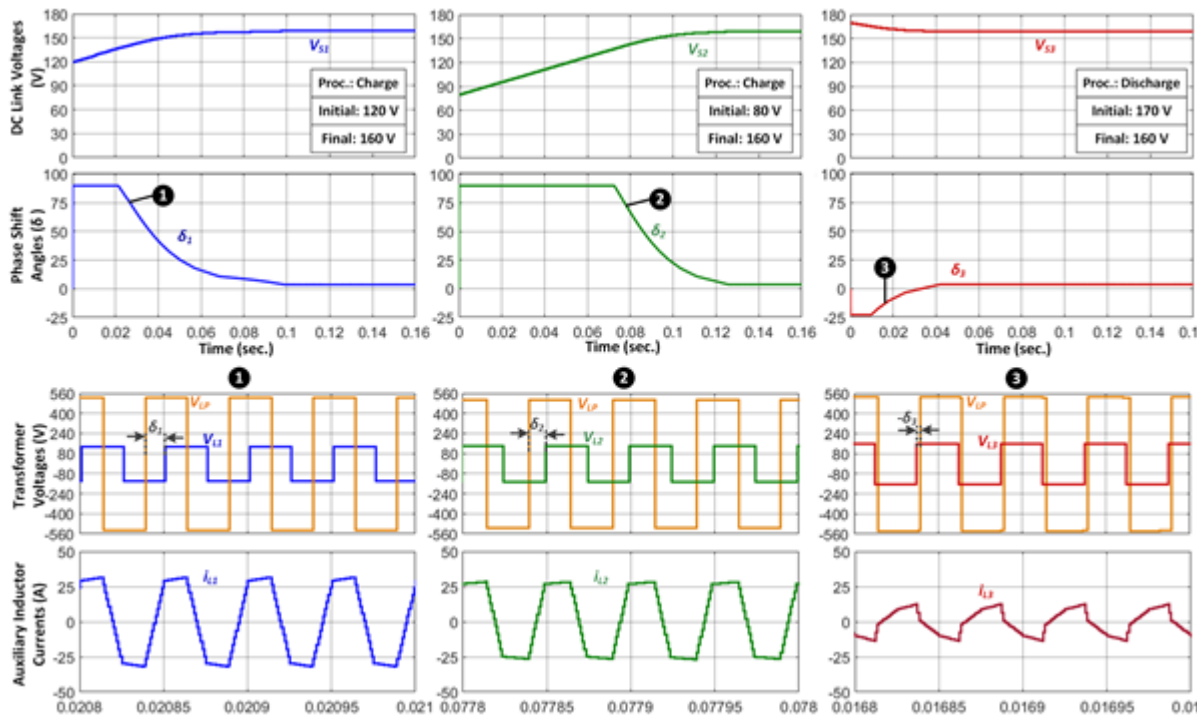


Fig. 5. The performance of the proposed system with SPS modulation.

The dynamical change of power flow is also investigated in the paper and Figure 6 shows the results of this state. As can be seen from Figure 6, the increase in the voltage of the dc link capacitor (V_{S1}) leads to a power transfer from the secondary side to the primary side. Because, the controller of the system aims to provide a constant voltage (160 V) in the dc links of the secondary. The power transfer to the primary side causes an increase in voltage of V_P . The instantaneous decrease in the voltage of V_{S1} causes an instantaneous change in the power transfer direction. Thus, V_P voltage decreases. The change of the phase shift angle at the time of changing the direction of power transfer is also indicated in the Figure 6.

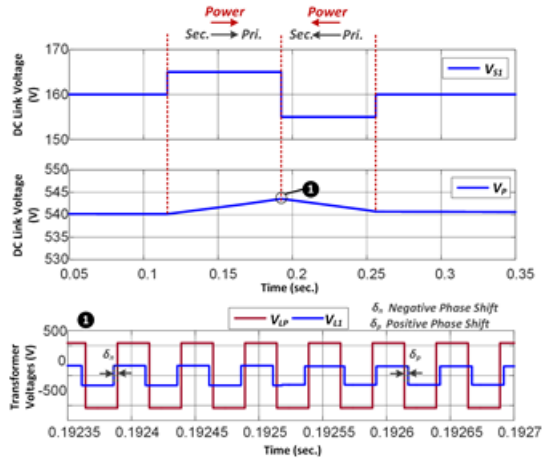


Fig. 6. The performance of the proposed system with SPS modulation

To improve the conversion efficiency of the proposed converter system by reducing the circulating current, the aforementioned modulation methods are applied to the controller. EPS and DPS modulation methods are typically improved techniques of SPS. In EPS modulation, the switch pairs of one side bridge have only outer phase shift angle, while the switch pairs of the other side bridge have both outer and inner phase shift angle. The output voltage of the primary side H bridge becomes three level while the output voltage of the secondary side H bridge is two level. In DPS modulation, the switch pairs of both side bridges have both outer and inner phase shift angle. The output voltage of the primary side H bridge becomes three level while the

output voltage of the secondary side H bridge is three level too. Thus, the voltage across the total inductance is three levels instead of two levels. This allows a reduction in circulating current (Zhao et al., 2014). Although EPS and DPS modulation methods improve the efficiency of the system and decrease the current stress, they limit the transferred power. So, the charging time of the dc links increases as understood from Figure 7. The comparison of the applied modulation techniques is presented in Figure 7.

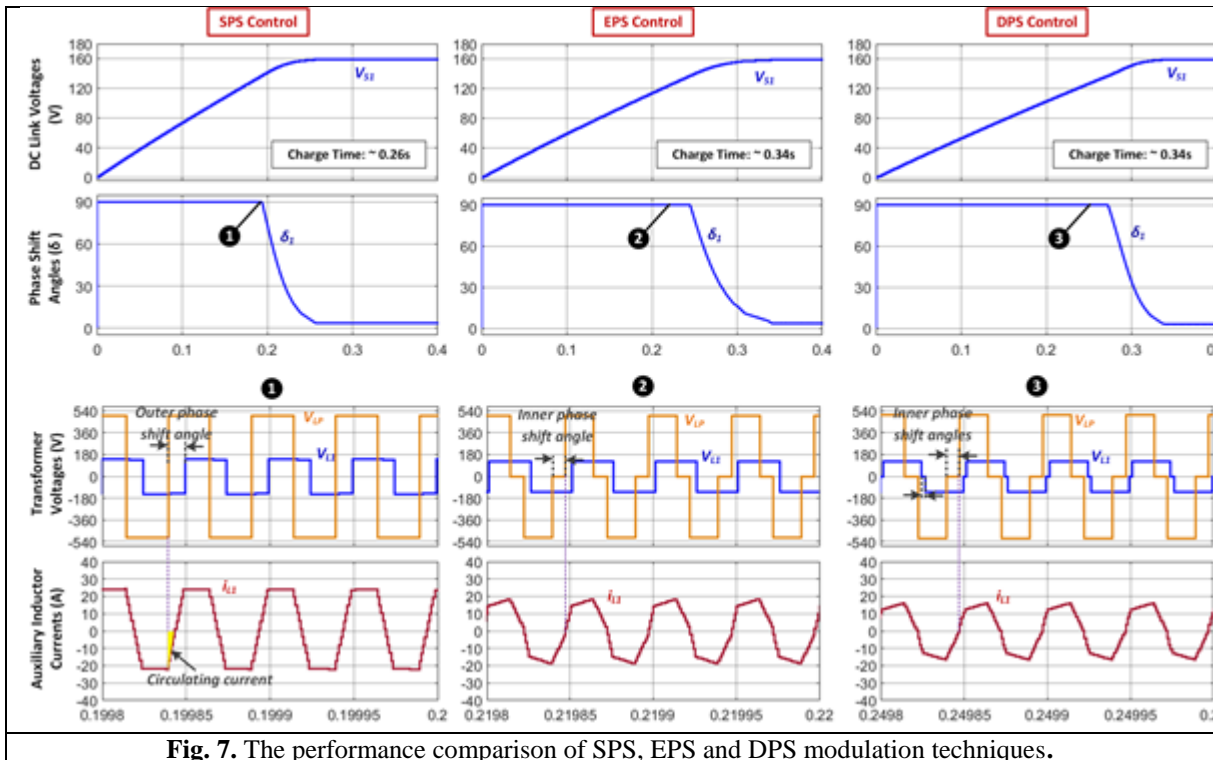


Fig. 7. The performance comparison of SPS, EPS and DPS modulation techniques.

5. Conclusion

A dual active bridge based bidirectional DC-DC converter topology equipped with an HFT with 1 primary 3 secondary windings has been proposed in this paper. The proposed converter allows providing galvanic isolation in the system by using HFT. Moreover, separate DC link capacitors also provide

isolation between the dc links. The proposed model also allows using small capacities for dc link capacitors by using separate dc link capacitors. The performance of the system is examined with a simulation model and validated by simulation results. As it can be seen from the results, the proposed system can provide bidirectional power flow and control secondary side dc links separately. The performance comparison of SPS, EPS and DPS modulation methods are also presented in the paper.

Acknowledgment

This study is supported by Cukurova University Scientific Research Projects Funding (Project Number: FBA-2017-7688).

References

- [1] Karshenas, H.R., Daneshpajoo, H., Safaei, A., Jain P., Bakhshai, A. "bidirectional dc-dc converters for energy storage systems", Chapter 8 in Energy Storage in the Emerging Era of Smart Grids, Edited by Prof. Rosario Carbone, 2011.
- [2] Zhao, C., Round, S.D., Kolar, J.W., 2008, "An isolated three-port bidirectional dc-dc converter with decoupled power flow management", IEEE Transactions on Power Electronics, 23(5), 2443-2453.
- [3] Ardi, H., Ahrabi, R.R., Ravadanegh, S.N., 2014, "Non-isolated bidirectional DC-DC converter analysis and implementation", IET Power Electronics, 7(12), 3033-3044.
- [4] Lin, C.C., Yang, L.S., Wu, G.W., 2012, "Study of a non-isolated bidirectional DC-DC converter", IET Power Electronics, 6(1), 30-37.
- [5] Tytelmaier, K., Husev, O., Veligorskyi, O., and Yershov, R., 2016, "A review of non-isolated bidirectional dc-dc converters for energy storage systems", International Young Scientists Forum on Applied Physics and Engineering.
- [6] Aggeler, D., Biela, J., Inoue, S., Akagi, H., 2007, "Bi-directional isolated dc-dc converter for next-generation power distribution – comparison of converters using Si and SiC Devices", Power Conversion Conference. 510-517.
- [7] Zhao, B., Song, Q., Liu, W., Sun, Y., 2014, "Overview of dual-active-bridge isolated bidirectional DC-DC converter for high-frequency-link power-conversion system", IEEE Transactions on Power Electronics, 29(8), 4091-4106.
- [8] Venkatesa, V., 1989, "Current mode controlled bidirectional flyback converter", Power Electronics Specialists Conference, 2, 835-842.
- [9] Chung, H.S.H., Cheung W.L., Tang, K.S., 2004, "A ZCS bidirectional flyback DC/DC converter", IEEE Transactions on Power Electronics, 19(6), 1426-1434.
- [10] Zhang, F., Yan, Y., 2009, "Novel forward-flyback hybrid bidirectional DC-DC converter", IEEE Transactions on Industrial Electronics, 56(5), 1578-1584.
- [11] Huber, L., Jovanovic, M.M., 1999, "Forward-flyback converter with current-doubler rectifier: analysis, design, and evaluation results", IEEE Transactions on Power Electronics, 14(1), 184-192.
- [12] Aboulnaga, A.A., Emadi, A., 2004, "Performance evaluation of the isolated bidirectional cuk converter with integrated magnetics", Annual IEEE Power Electronics Specialists Conference, 1557-1562.
- [13] Li, H., Peng, F.Z., Lawler, J.S., 2003, "A natural ZVS medium-power bidirectional DC-DC converter with minimum number of devices", IEEE Transactions on Industry Applications, 39(2), 525-535.
- [14] Peng, F.Z., Li, H., Su, G.J., Lawler, J.S., 2004, "A new ZVS bidirectional DC-DC converter for fuel cell and battery application", IEEE Transactions on Power Electronics, 19(1), 54-65.
- [15] Naayagi, R.T., Forsyth, A.J., Shuttleworth, R., 2012, "High-power bidirectional DC-DC converter for aerospace applications", IEEE Transactions on Power Electronics, 27(11), 4366-4379.
- [16] Mi, C., Bai, H., Wang, C., Gargies, S., 2008, "Operation, design and control of dual H-bridge-based isolated bidirectional DC-DC converter", IET Power Electronics, 1(4), 507-517.
- [17] Bai, H., Mi, C., 2008, "Eliminate reactive power and increase system efficiency of isolated bidirectional dual-active-bridge DC-DC converters using novel dual-phase-shift control", IEEE Transactions on Power Electronics, 23(6), 2905-2914.
- [18] Inoue, S., Akagi, H., 2007, "A bi-directional DC/DC converter for an energy storage system", Annual IEEE Applied Power Electronics Conference, 761-767.
- [19] Somayajula, D., Mariesa, L., 2015, "An integrated dynamic voltage restorer-ultracapacitor design for improving power quality of the distribution grid", IEEE Transactions on Sustainable Energy, 6(2), 616-624.
- [20] Somayajula, D., Mariesa, L., 2014, "An ultracapacitor integrated power conditioner for intermittency smoothing and improving power quality of distribution grid", IEEE Transactions on Sustainable Energy, 5(4), 1145-1155.

- [21] Goharrizi, A.Y., Hossein, S.H., Sabahi, M., Gharehpetian, G.B., 2012, "Three-phase hfl-dvr with independently controlled phases", *IEEE Transactions on Power Electronics*, 24(4), 1706-1718.
- [22] Cheng, K.W.E., Ho, S.L., Wong, K.P., Cheung, T.K., and Ho, Y.L., 2006, "Examination of square-wave modulated voltage dip restorer and its harmonics analysis", *IEEE Transactions on Energy Conversion*, 21(3), 759-766.
- [23] Inci, M., Bayindir, K.C., Tumay, M., 2017, "The performance improvement of dynamic voltage restorer based on bidirectional dc-dc conerter", *Electrical Engineering*, 99(1), 285-300.
- [24] Jimichi, T., Fujita, H., Akagi, H., 2008, "Design and experimentation of a dynamic voltage restorer capable of significantly reducing an energy-storage element", *IEEE Transactions on Industry Applications*, 44(3), 817-825.
- [25] Jimichi, T., Fujita, H., Akagi, H., 2011, "A dynamic voltage restorer equipped with a high-frequency isolated dc-dc converter", *IEEE Transactions on Industry Applications*, 47(1), 169-175.
- [26] Nadia, M.L., Inoue, S., Kobayashi, A., and Akagi, H., 2008, "Voltage balancing of a 320-V, 12-F electric double layer capacitor bank combined with a 10-kW bidirectional isolated DC-DC converter", *IEEE Transactions on Power Electronics*, 23(6), 2755-2765.
- [27] Zhao, B., Yu, Q., and Sun, W., 2012, "Extended-phase-shift control of isolated bidirectional DC-DC converter for power distribution in microgrid", *IEEE Transactions on Power Electronics*, 27(11), 4667-4680.
- [28] Zhao, B., Song, Q., and Liu, W., 2012, "Power characterization of isolated bidirectional dual-active-brdige DC-DC converter with dual-phase-shift control", *IEEE Transactions on Power Electronics*, 27(9), 4172-4176.
- [29] Bai, H., Nie, Z., and Mi, C., 2010, "Experimental comparison of traditional phase-shift, dual-phase-shift, and model-based control of isolated bidirectional dc-dc converters", *IEEE Transactions on Power Electronics*, 25(6), 1444-1449.